Supplementary Information

Structural basis for diverse *N*-glycan recognition by HIV-1-neutralizing V1V2-directed antibody PG16

Marie Pancera, Syed Shahzad-ul-Hussan, Nicole A. Doria-Rose, Jason S. McLellan, Robert T. Bailer, Kaifan Dai, Sandra Loesgen, Mark K. Louder, Ryan P. Staupe, Yongping Yang, Baoshan Zhang, Robert Parks, Joshua Eudailey, Krissey E. Lloyd, Julie Blinn, S. Munir Alam, Barton F. Haynes, Mohammed N. Amin, Lai-Xi Wang, Dennis R. Burton, Wayne C. Koff, Gary J. Nabel, John R. Mascola, Carole A. Bewley and Peter D. Kwong

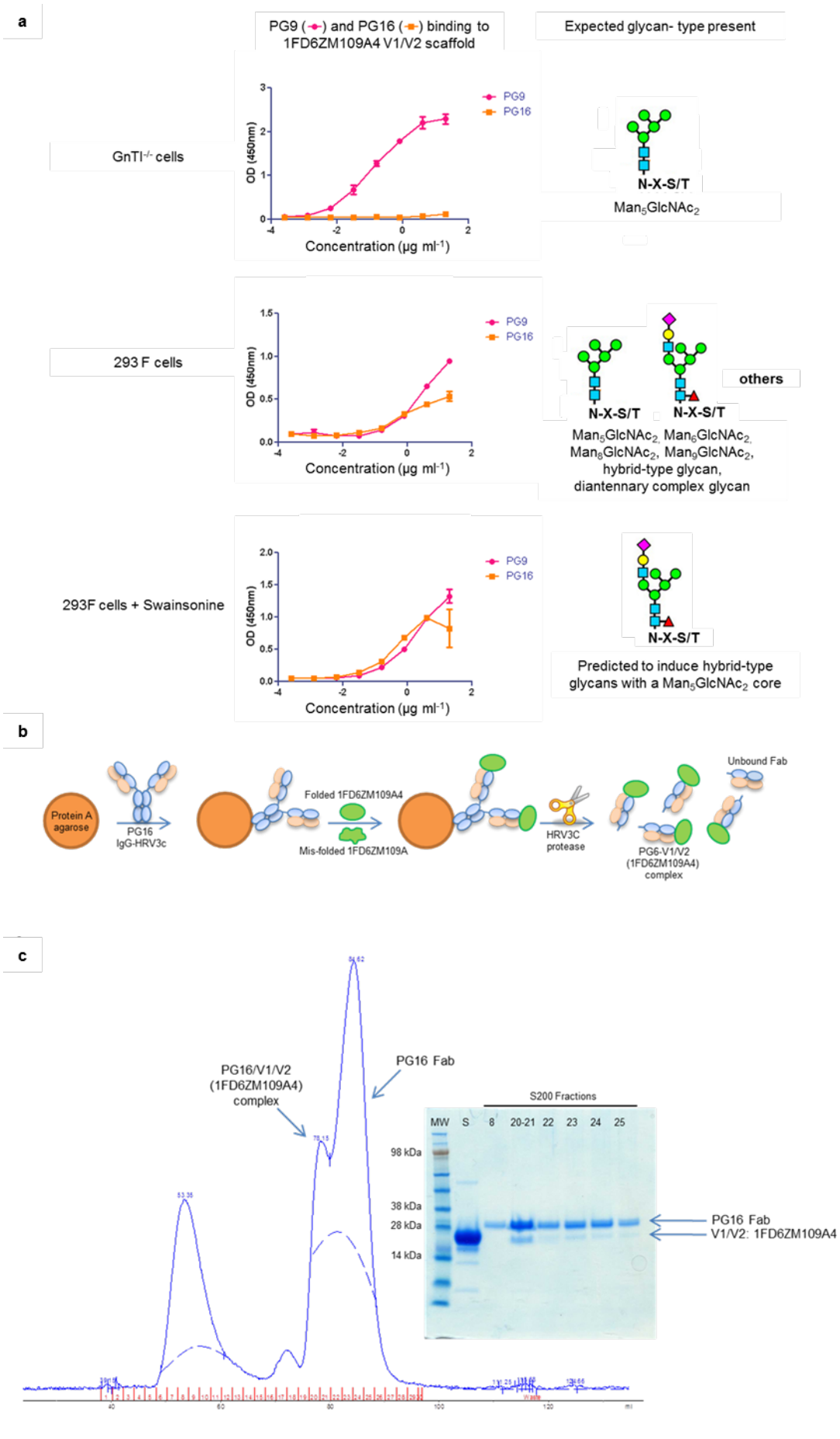
a
PG9 (●) and PG16 (■) binding to 1FD6ZM109A4 V1/V2 scaffold
Expected glycan- type present
GnTI-/- cells
OD (450nm)
Concentration (μg ml-1)
PG9
PG16
N-X-S/T
Man5GlcNAc2
293 F cells
others
Man5GlcNAc2, Man6GlcNAc2, Man8GlcNAc2, Man9GlcNAc2, hybrid-type glycan, diantennary complex glycan
293F cells + Swainsonine
Predicted to induce hybrid-type glycans with a Man5GlcNAc2 core
b
Protein A agarose
PG16 IgG-HRV3c
Folded 1FD6ZM109A4
Mis-folded 1FD6ZM109A
HRV3C protease
Unbound Fab
PG6-V1/V2 (1FD6ZM109A4) complex
c
PG16/V1/V2 (1FD6ZM109A4) complex
PG16 Fab
S200 Fractions
MW
S
8
20-21
22
23
24
25
98 kDa
38 kDa
28 kDa
14 kDa
PG16 Fab
V1/V2: 1FD6ZM109A4

Supplementary Figure 1 | 1FD6ZM109V1/V2 scaffold binding to PG16: characterization and purification. a, ELISA Binding of PG9 and PG16 to V1/V2 scaffolds expressed in different cell lines. ELISA binding of PG9 (pink) and PG16 (orange) to scaffolded V1/V2 from strain ZM109 expressed in $GnTI^{-/-}$ cells (enriched in $Man_5GlcNAc_2$ glycans), 293F cells or 293F cells with swainsonine added after transfection (enriched in hybrid-type glycans). On-column complex formation and purification shown in **b, c**. **b**, Schematic showing the on-column complex formation between PG16 and scaffolded 1FD6ZM109A4 V1/V2s, as described in Methods. **c**, Gel filtration result of the elution shown in a. A coomassie blue-stained SDS-PAGE gel is shown for fractions as indicated on the gel. MW=molecular weight standards. S = purified scaffolded V1/V2 1FD6 ZM109A4. 8 mgs of scaffolded V1/V2 1FD6ZM109A4 was used to obtain 200µgs of complex PG16/V1/V2(1FD6ZM109A4).

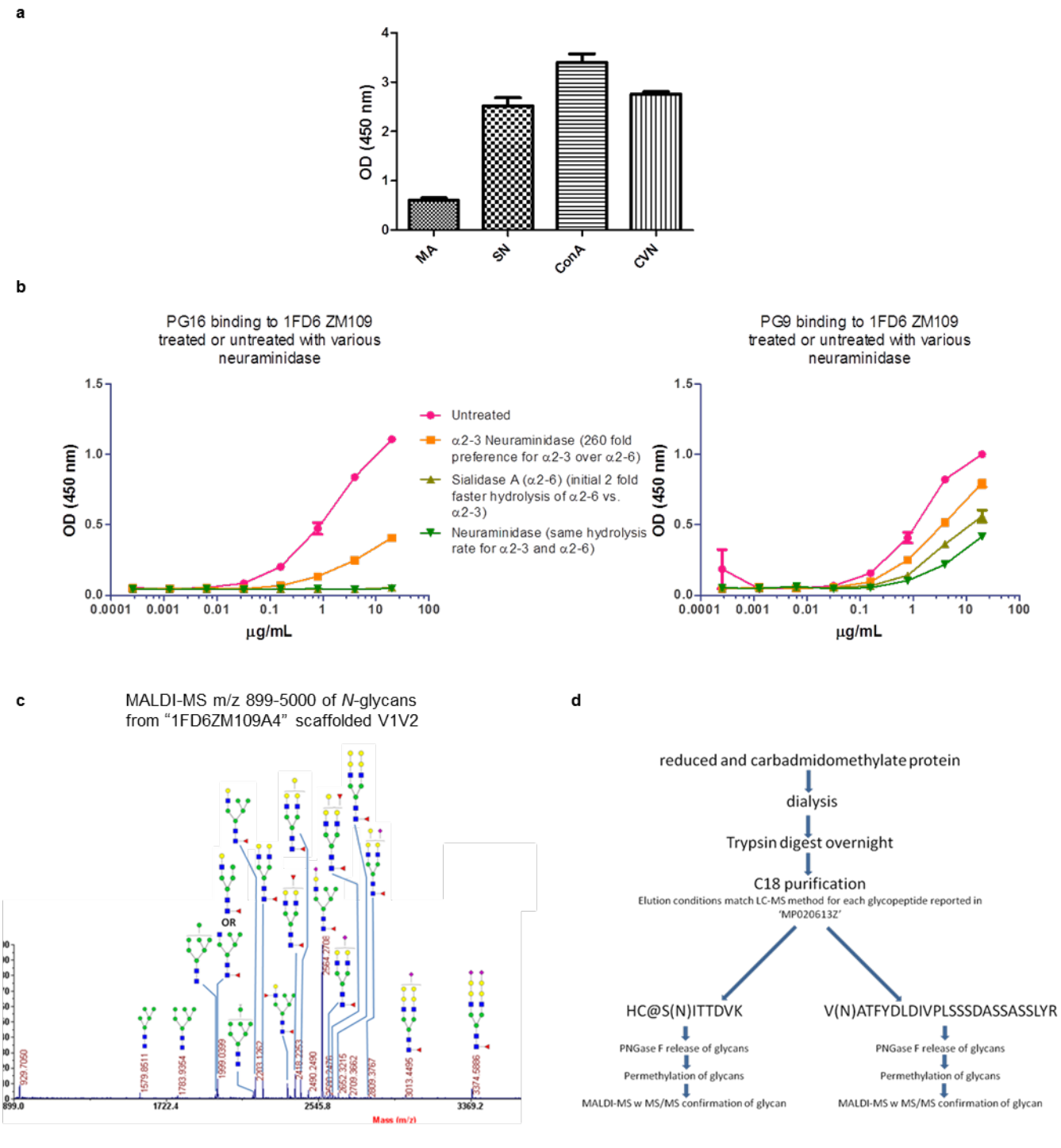
a
OD (450 nm)
MA
SN
ConA
CVN
b
PG16 binding to 1FD6 ZM109 treated or untreated with various neuraminidase
PG9 binding to 1FD6 ZM109 treated or untreated with various neuraminidase
OD (450 nm)
µg/mL
Untreated
α2-3 Neuraminidase (260 fold preference for α2-3 over α2-6)
Sialidase A (α2-6) (initial 2 fold faster hydrolysis of α2-6 vs. α2-3)
Neuraminidase (same hydrolysis rate for α2-3 and α2-6)
c
MALDI-MS m/z 899-5000 of N-glycans from "1FD6ZM109A4" scaffolded V1V2
OR
Mass (m/z)
d
reduced and carbadmidomethylate protein
dialysis
Trypsin digest overnight
C18 purification
Elution conditions match LC-MS method for each glycopeptide reported in 'MP020613Z'
HC@S(N)ITTDVK
V(N)ATFYDLDIVPLSSSDASSASSLYR
PNGase F release of glycans
Permethylation of glycans
MALDI-MS w MS/MS confirmation of glycan

e

Observed m/z	Proposed Structure	Proposed Figure	% Peak Area Fraction $N160_{gp120}$ "HC@S(N)IT TDVK"	% Peak Area Fraction $N173_{gp120}$ "V(N)ATFYDL DIVPLSSSDA SSASSLYR"
1579.9	(GlcNAc)2(Man)5		20	9
1783.9	(GlcNAc)2(Man)6		6	2
1988.1	(GlcNAc)2(Man)7		5	2
1999.0	(GlcNAc)3(Man)5 (Fuc) OR (GlcNAc)3(Man)4(Gal)(Fuc)	or	9	6
2192.1	(GlcNAc)2(Man)8		3	2
2203.1	(GlcNAc)3(Man)5(Gal)(Fuc)		7	4
2244.2	(GlcNAc)4(Man)3(Gal)(Fuc)		4	3
2377.2	(GlcNAc)3(Man)5(Gal)(Fuc)2		5	3
2418.2	(GlcNAc)4(Man)3(Gal)2(Fuc)2		5	4
2448.2	(GlcNAc)4(Man)3(Gal)3(Fuc)2		2	1
2564.3	(GlcNAc)3(Man)5(Gal)(Fuc)(NeuAc)		30	56
2605.3	(GlcNAc)4(Man)3(Gal)2(Fuc)(NeuAc)		3	6
2622.3	(GlcNAc)4(Man)3(Gal)3(Fuc)2		0	0
2652.3	(GlcNAc)4(Man)3(Gal)4(Fuc)		0	1
2809.4	(GlcNAc)4(Man)3(Gal)3(Fuc)(NeuAc)		0	0
3013.4	(GlcNAc)4(Man)3(Gal)4(Fuc)(NeuAc)		0	0
3374.6	(GlcNAc)4(Man)3(Gal)4(Fuc)(NeuAc)2		0	0
	Total		100	100

f

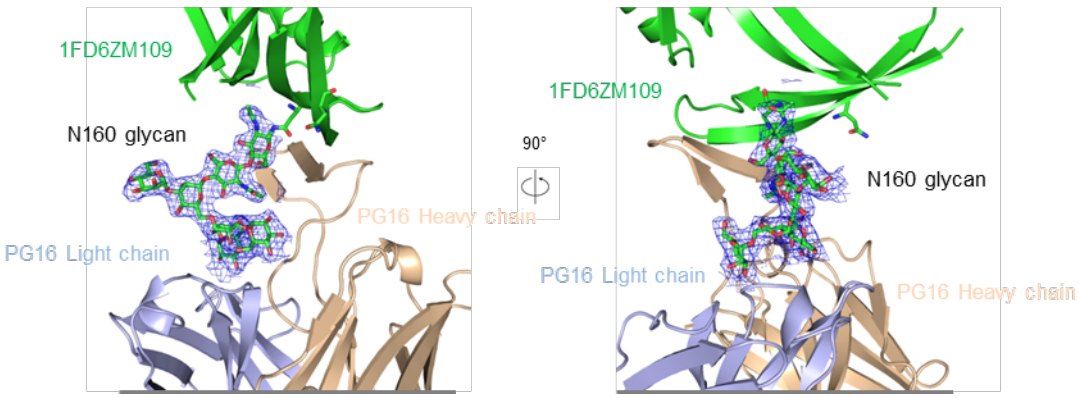

Supplementary Figure 2 | Glycoforms present on the scaffolded V1/V2 1FD6 ZM109 A4.
a, ELISA binding of selected lectins including *Maackia amurensis* lectin II (MA), *Sambucus nigra* lectin (SN), concavalin A (ConA) and cyanovirin-N (CVN) to scaffolded V1/V2. **b**, ELISA showing binding of PG9 and PG16 to 1FD6 V1/V2 ZM109 A4 scaffold, either untreated or treated with various neuraminidases (3 hours at 37°C per manufacturer's instruction) that show different specificities for the linkage between galactose and sialic acid. PG16 does not bind to scaffolded V1/V2 pretreated with

neuraminidase or Sialidase A (faster rate for α2-6 linkage) but retains binding to scaffold treated with α2-3 neuraminidase. PG9 is less affected by neuraminidase treatment. 1FD6 ZM109 A4 scaffold was either untreated or treated with various neuraminidases per manufacturer's instructions for 3 hours at 37 °C. α2-3 Neuraminidase is a highly specific exoglycosidase that catalyzes the hydrolysis of α2-3 and, at a much lower rate, α2-6 linked N-acetyl-neuraminic acid residues from oligosaccharides. This enzyme has a 260-fold preference for α2-3 sialyl linkages over α2-6 sialyl linkages and shows only trace activity against α2-8 sialyl linkages. Sialidase A releases α2-3-, α2-6-, α2-8- and α2-9-linked N-acetylneuraminic acid from complex carbohydrates. The initial rate of hydrolysis of α2-6 linkages is reported to be approximately twice that of α2-3-linked sialic acid however, in practice, this kinetic selectivity is of little consequence during extended incubations (Uchida et al., 1979). **c**, MALDI MS analysis of *N*-glycans released from 1FD6ZM109A4 with detection covering *m*/*z* 899-5000. **d**, Overview of sample processing. (**e**) Proposed *N*-linked glycans assigned on the basis of molecular weight, and their percent abundance. Glycan analyses and glycopeptide mapping were performed at the Complex Carbohydrate Research Center. Experimental details are freely available at http://www.ccrc.uga.edu/services/ccrcanalyticalservices/index.html. **e**, $Man_5GlcNAc_2$ electron density. $Man_5GlcNAc_2$ and Asn160 are shown in green stick representation why oxygen atoms in red and nitrogen atoms in blue. Scaffolded-V1V2 is shown in green ribbon representation as well as PG16 antibody (heavy chain is tan and light chain is light blue).The 2Fo-Fc map obtained after final refinement is shown in blue at 1σ.

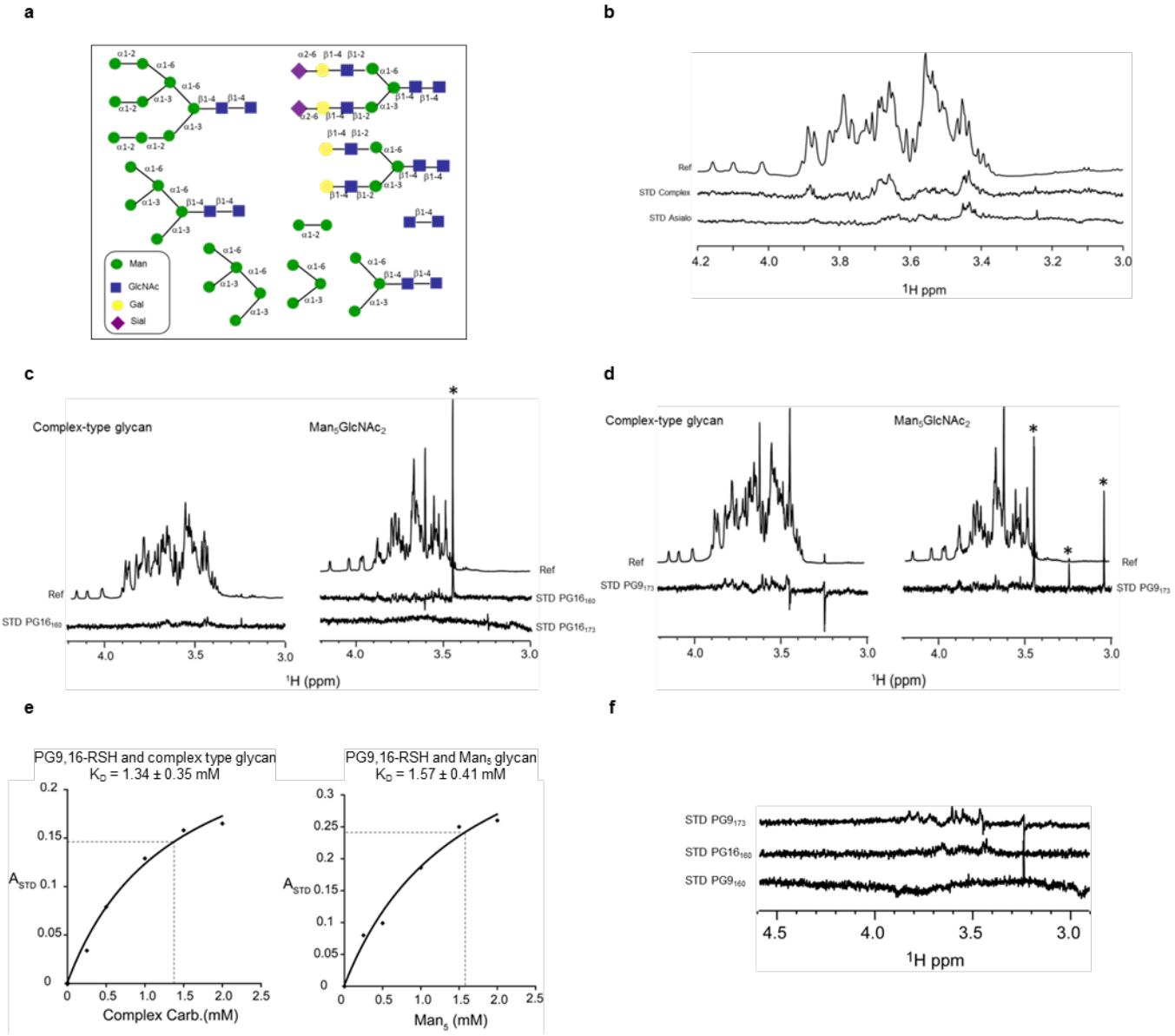

Supplementary Figure 3 | NMR data.

a, Glycan fragments from gp120 used for screening. Glycan fragments shown are representative of those present on gp120. Each of these glycans was analyzed by STD NMR for binding to PG16 and PG9 antibodies. **b**, Complex-type glycan binds PG16 mainly through terminal sialic acids. STD NMR spectra of 2 mM complex-type glycan (middle) and 2 mM asialo complex-type glycan (bottom) in the presence of 20 μM Fab PG16. **c**, $Man_5GlcNAc_2$ binds negligibly to $PG16_{160}$ and does not bind to $PG16_{173}$, complex-type glycan binds negligibly to $PG16_{160}$. Left panel, STD (lower) and corresponding reference (upper) spectra of 2 mM complex-type glycan in the presence of 20 μM $PG16_{160}$ shows negligible STD enhancements. Right panel, STD NMR spectra of 2 mM $Man_5GlcNAc_2$ in the presence of 20 μM $PG16_{173}$ (lowest) shows no binding and 20 μM PG16160 (middle) shows negligible binding. The corresponding reference spectrum is shown at the top. **d**, $PG9_{173}$ binds complex-type glycan very weakly and $Man_5GlcNAc_2$ negligibly. STD and corresponding reference spectra of 2 mM complex-type glycan (left panel) and 2 mM $Man_5GlcNAc_2$ in the presence of 20 μM $PG9_{173}$(right panel). The signal denoted by an asterisk (*) corresponds to a buffer impurity. **e**, Binding curves used to calculate the K_Ds

of chimeric antibody PG9,16-RSH to complex-type glycan and $Man_5GlcNAc_2$. Langmuir binding curves showing the effects on STD enhancement (expressed as the STD amplification factor $A_{\mathbf{STD}}$) as a function of glycan concentration at a saturation time of 0.2 s ($t_{\mathbf{sat}}$=0.2 s), and used to obtain the equilibrium dissociation constants (K_D) from the initial slopes. **f**, Qualitatively defined very weak and negligible binding affinities. STD NMR spectra of 2 mM complex-type glycan in the presence of 20 μM PG16 and PG9 mutants. Complex-type glycan binds to $PG9_{173}$ very weakly (upper) and to $PG16_{160}$ negligibly (middle). This glycan does not bind to $PG9_{160}$ (lower).

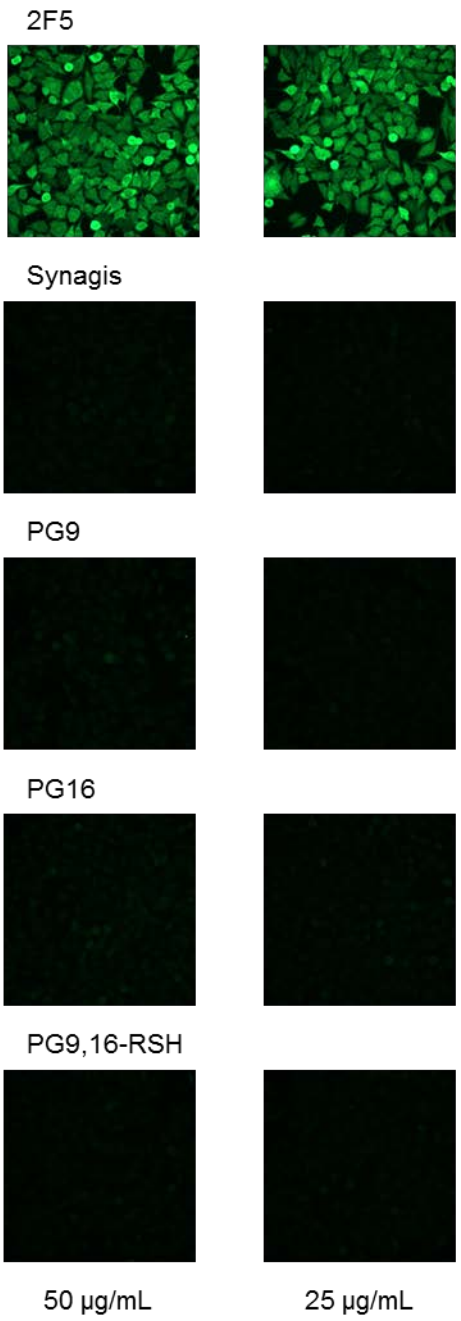

Cardiolipin reactivity

	concentration (µg/ml)							
Antibody	100	33.33	11.11	3.70	1.23	0.41	0.14	0.05
PG9	0.079	0.049	0.044	0.039	0.042	0.039	0.041	0.041
PG16	0.711	0.296	0.079	0.046	0.042	0.039	0.041	0.034
PG9,16-RSH	0.511	0.116	0.065	0.044	0.042	0.040	0.041	0.041
Synagis	0.040	0.039	0.039	0.039	0.040	0.038	0.041	0.042
4E10 IgG1	2.612	2.587	2.478	2.198	1.761	0.999	0.456	0.187

Athena antinuclear antigen reactivity

Antibody	ug/ml	Autoantigen								
		SSA	SSB	Sm	RNP	Scl 70	Jo 1	dsDNA	Cent B	Histone
PG9	50	3	2	5	5	3	3	25	5	6
	25	3	2	2	3	2	2	12	2	3
	12.5	1	3	4	3	3	4	10	1	4
	6.25	2	2	3	2	3	2	8	1	3
PG16	50	4	3	5	5	4	2	1	2	0
	25	3	4	4	3	4	2	10	2	2
	12.5	1	3	3	3	3	3	6	1	2
	6.25	2	2	4	2	1	3	5	1	2
PG9,16-RSH	50	4	2	9	2	10	9	30	3	2
	25	3	2	5	3	5	5	26	2	1
	12.5	3	2	2	1	3	4	17	2	4
	6.25	2	2	4	2	3	2	19	2	2
Synagis	50	3	3	4	3	2	2	7	1	3
	25	3	2	4	2	2	3	1	1	2
4E10 IgG1	50	201	276	21	7	3	204	17	57	140
	25	155	249	14	4	2	182	8	34	110
Neg Control	-	-	-	-	-	-	-	-	-	-
Pos Control 1	-	650	435						204	
Pos Control 2							539	1051		752
Pos Control 3				701	420	421				
Neg Control	-	-	-	-	-	-	-	-	-	-

Supplementary Figure 4 | Autoreactivity assessment of PG9, PG16 and PG9,16-RSH.
Immunofluorescence of HEp-2 epithelial cells stained with antibody at 50 and 25 µg/ml. Cardiolipin reactivity: samples for which cardiolipin reactivity exceeded 0.2 are highlighted in yellow. Athena antinuclear antigen reactivity: samples for with autoantigen reactivity exceeded 125 are highlighted in yellow.

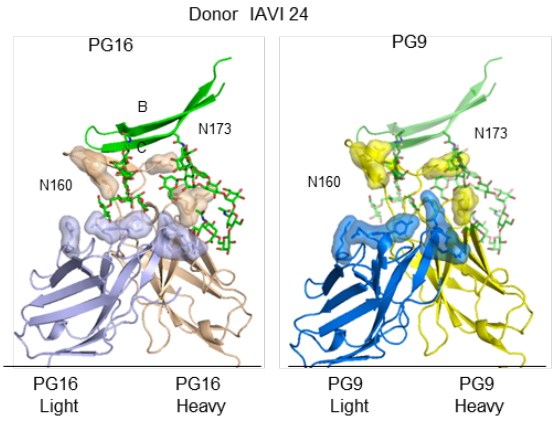

20.0% of somatic changes that result in different residues between PG16 and PG9 interact with glycans, 27.3% interact with both protein and glycans

Germline	PG16	Glycans	PG9	Glycans
H SER 55	H MET 55	Not determined	H SER 55	156/173 NAG 657, MAN 658, 659
H ASN 56	H ARG 56	156/173, SIA 582	H GLU 56	Not determined
CDR H3 insertion	H ILE 100	160, NAG 561, MAN 565	H ASP 100	160, NAG 560, 561, MAN 565
CDR H3 insertion	H HIS 100B	160, NAG 560, 561	H ARG 100B	160, NAG 560, 561
H TRP 100K	H ASN 100K	156/173, NAG 573	H TYR 100K	156/173, NAG 657, 160, MAN 660, 662
L TYR 30	L PHE 30	160, MAN 562, 564, 566	L TYR 30	160, MAN 562, 564, 566
L ASN 31	L ASP 31	160, MAN 564, 565	L GLU 31	160, MAN 564, 565
L ASN 53	L HIS 53	Not determined	L LYS 53	160, MAN 565
L SER 94	L ARG 94	156/173, GAL 581, SIA 582	T L HR 94	Not determined
L SER 95	L SER 95	160, MAN 566, 156/173, MAN 578	L ARG 95	160, MAN 566
L THR 95A	L HIS 95A	156/173, SIA 582	L ARG 95A	Not determined

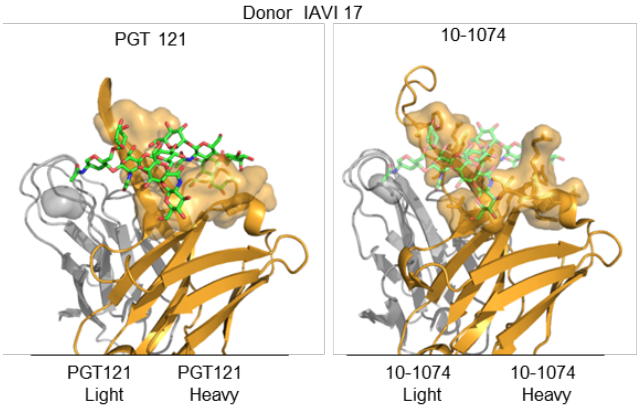

22.3% of somatic changes that result in different residues between PGT121 and 10-1074 interact with glycans

Germline	PGT121	Glycans	10-1074	Glycans
H SER 31	H ASP 31	SIA 310, GAL 308	H ASN 31	Not determined
H TYR 32	H SER 32	SIA 310	H TYR 32	Not determined
H TYR 52	H HIS 52	NAG 307, GAL 308	H SER 52	Not determined
H TYR 53	H LYS 53	GAL 308	H ASP 53	Not determined
H SER54	H SER 54	NAG 307, GAL 308	H ARG 54	Not determined
H GLU 55	H GLY 55	NAG 304, BMA 301, MAN 303	H GLU 55	Not determined
H SER 56	H ASP 56	NAG 307, MAN 302, BMA 301	H SER 56	Not determined
H THR 57	H THR 57	NAG 304, MAN 303	H ALA 57	Not determined
H ASN 58	H ASN 58	NAG 304, 306 BMA 301, MAN 303,	H THR 58	Not determined
H GLN 97	H HIS 97	NAG 307, GAL 308	H ARG 97	Not determined
H LYS 99	H ARG 99	NAG 307, MAN 302	H GLN 99	Not determined
H TYR 100J	H TRP 100J	MAN 302	H PHE 100J	Not determined
H TYR 100L	H THR 100L	NAG 307, MAN 302	H TYR 100L	Not determined
H TYR 100O	H TYR 100O	SIA 310	H SER 100O	Not determined
L ASP 95A	L PRO 95A	NAG 305	L GLY 95A	Not determined

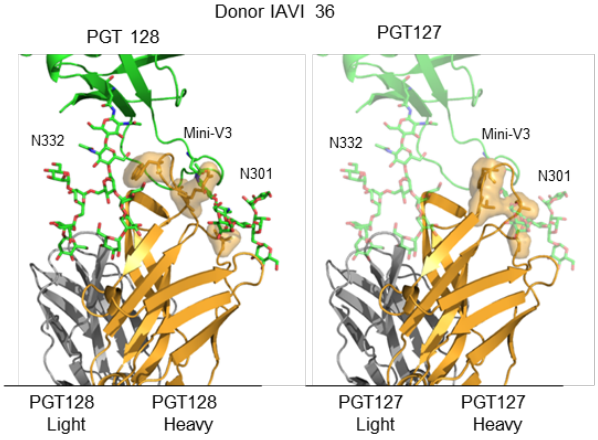

19.0% of somatic changes that result in different residues between PGT128 and PGT127 interact with glycans, 33.3% interact with both protein and glycans

Germline	PGT128	Glycans	PGT127	Glycans
H SER 30	H ALA 30	NAG 2 (cpx)	H GLY 30	Not determined
H GLY 52C	H ALA 52C	NAG 1 (cpx)	H ARG 52C	Not determined
CDR H2 insertion	H TRP 52F	MAN 4 (man9), NAG 2 (cpx)	H TYR 52F	Not determined
HCDR H2 insertion	H ARG 54	MAN D3 (man9), MAN 4 (cpx)	H THR 54	Not determined

Supplementary Figure 5 | Glycan interactions with various somatic variants.
Somatic variants for donor IAVI 24 (PG16, PG9), IAVI 17 (or patient 10) (PGT121, 10-1074), IAVI 36 (PGT128, PGT127) are shown in cartoon representation (with heavy and light chain in different colors) bound to glycans (green sticks, transparent when modeled). Residues that are affinity matured and differed between somatic variants are shown as sticks and semitransparent surface representation and are listed. The percentages of somatic changes that interact with glycans only or with both proteins and glycans are indicated.

Supplementary Table 1. Comparison of glycan specificities of anti-gp120 glycan directed antibodies

Anti-gp120 antibody	glycan specificity	References
2G12	Manα1-2Man (of $Man_{8-9}GlcNAc2$)	Calarese et al., 2003, Science
PGT125-130	$Man_{8-9}GlcNAc_2$	Walker et al., 2011, Nature
PGT121	Complex-type glycan	Walker et al., 2011, Nature; Mouquet et al., PNAS, 2012
PGT141-144	$Man_5GlcNAc_2$	Walker et al., 2011, Nature
PGT145	$Man_9GlcNAc_2$	Walker et al., 2011, Nature
PG9	$Man_5GlcNAc_2$ (N160 site)	Walker et al., 2009, Science; McLellan et al., 2011, Nature
CH01-CH05	$Man_5GlcNAc_2$	Bonsignori et al., 2011, J. Virol.

Supplementary Table 2. ZM109: PG16 interactions

A. ZM109-Protein : PG16-Protein interactions

	Interface Residue	Bond Type	ASA	BSA	$\Delta_i G$
	ZM109:SER 158		32.30	1.00 |	0.02
	ZM109:ASN 160		75.57	22.91 ||||	-0.07
	ZM109:THR 163		38.97	3.99 ||	-0.03
	ZM109:LYS 166		156.02	4.06 |	-0.05
ZM109	ZM109:ASP 167	H	112.64	62.08 ||||||	0.04
	ZM109:ARG 168	HS	150.62	101.40 |||||||	-1.21
	ZM109:LYS 169	H	110.83	75.27 ||||||	0.32
	ZM109:GLN 170		93.97	66.16 |||||||	0.04
	ZM109:LYS 171	H	147.63	89.15 ||||||	0.22
	ZM109:VAL 172		40.63	4.66 ||	0.07
	ZM109:ASN 173		126.70	22.32 ||	-0.13
	H:TRP 100A		141.19	0.31 |	0.00
	H:ASP 100C		133.63	10.68 |	-0.12
	H:ASP 100D		132.70	15.19 ||	-0.16
	H:VAL 100E		69.35	54.79 |||||||	0.88
	H:LYS 100F	H	84.96	49.90 ||||||	0.07
PG16	H:TYR 100G		101.40	59.23 ||||||	0.72
	H:TYS 100H	H	115.35	69.49 ||||||	-0.23
	H:ASP 100I		53.65	15.65 |||	-0.08
	H:PHE 100J		178.64	94.07 ||||||	1.45
	H:ASN 100K		151.68	16.90 ||	0.03
	H:ASP 100L	HS	108.53	59.62 ||||||	-0.46
	H:TYR 100O		80.51	18.82 |||	-0.14

Bond type: H: **H**ydrogen, S: **S**alt bridge
ASA Accessible Surface Area, $Å^2$
BSA BuriedSurfaceArea,$Å^2$
$\Delta_i G$ Solvation energy effect, kcal/mol
|||| Buried area percentage, one bar per 10%
Detailed interface data was calculated on the EBI PISA server (http://www.ebi.ac.uk/msd-srv/prot_int/cgi-bin/piserver)

B. ZM109-Glycan160: PG16-Protein interactions

Interface Residue	Bond Type	ASA	BSA	$\Delta_i G$
ZM109:NAG 560-PG16:H	H	361.50	98.97 |||	-1.75
H:ILE 100		60.92	4.36 |	0.07
H:HIS 100B	H	102.12	15.83 ||	-0.34
H:TYR 100G		101.40	25.36 |||	0.41
H:TYR 100O		80.51	18.20 |||	-0.05
ZM109:NAG 561-PG16:H		360.36	75.68 |||	-2.26
H:ILE 100		60.92	16.40 |||	0.26
H:HIS 100B		102.12	8.46 |	-0.31
H:TYR 100O		80.51	21.05 |||	0.29
ZM109:MAN 562-PG16:L		292.34	10.70 |	-0.35
L:PHE 30		67.36	9.68 ||	0.15
ZM109:MAN 564-PG16:H		287.55	38.89 ||	-0.26
H:ILE 100		60.92	9.37 ||	0.15
H:TYR 100O		80.51	1.64 |	0.03
H:ASN 100P		71.09	0.37 |	-0.00
H: HIS 100R		155.46	29.58 ||	0.77
ZM109:MAN 564-PG16:L		287.55	47.13 ||	-0.61
L:PHE 30		67.36	21.88 ||||	0.35
L:ASP 31		100.74	7.10 |	0.06
L:SER 32		38.08	5.50 ||	-0.06
L:LEU 91		45.80	9.11 ||	0.15
ZM109:MAN 565-PG16:H	H	289.33	98.24 ||||	-0.57
H:ILE 100		60.92	29.97 |||||	0.48
H:HIS 100B		102.12	0.31 |	0.01
H:ASN 100P		71.09	2.92 |	-0.03
H:TYR 100Q		77.59	15.43 ||	0.04
H:HIS 100R	H	155.46	22.27 ||	0.01
ZM109:MAN 565-PG16:L	H	289.33	95.63 ||||	-1.91
L:ASP 31		100.74	21.19 |||	0.11
L:SER 32	H	38.08	12.37 ||||	-0.09
L:ASP 50		59.28	31.59 ||||||	-0.16
ZM109:MAN 566-PG16:H	H	291.89	111.31 ||||	-1.22
H:ASP 100I		53.65	0.25 |	-0.00
H:TYR 100O		80.51	20.81 |||	0.33
H:ASN 100P	H	71.09	22.59 ||||	-0.23
H:HIS 100R	H	155.46	27.12 ||	0.54
ZM109:MAN 566-PG16:L		291.89	66.07 |||	-1.11
L:PHE 30		67.36	9.99 ||	0.16
L:LEU 91		45.80	17.64 ||||	0.28
L:THR 92		19.83	0.73 |	-0.01
L:SER 95		90.99	16.90 ||	-0.17
L:ARG 96		174.64	4.07 |	-0.15

Bond type: H: **H**ydrogen, S: **S**alt bridge
ASA Accessible Surface Area, $Å^2$
BSA BuriedSurfaceArea,$Å^2$
$\Delta_i G$ Solvation energy effect, kcal/mol
|||| Buried area percentage, one bar per 10%
Detailed interface data was calculated on the EBI PISA server (http://www.ebi.ac.uk/msd-srv/prot_int/cgi-bin/piserver)

C. ZM109-Glycan173: PG16-Protein interactions

Interface Residue	Bond Type	ASA	BSA	$\Delta_i G$
ZM109:NAG 573-PG16:H		359.11	68.75 ||	-2.03
H:PHE 100J		178.64	54.27 ||||	0.87
H:ASN 100K		151.68	7.61 |	-0.13
ZM109:MAN 578-PG16:L		289.45	12.91 |	-0.38
L:ASP 93		89.43	2.95 |	-0.03
L:SER 95		90.99	10.80 ||	-0.12
ZM109:GAL 581-PG16:H		291.06	87.28 |||	-1.90
H:HIS 59		47.52	7.04 ||	-0.09
H:ASP 61		141.69	14.30 ||	-0.16
H:TRP 64		191.71	59.08 ||||	0.61
ZM109:GAL 581-PG16:L	H	291.06	18.46 |	0.43
L:ARG 94	H	168.75	17.83 ||	-0.40
ZM109:SIA 582-PG16:H	H	436.88	175.71 |||||	-0.61
H:ARG 56		119.07	13.22 ||	0.21
H:LYS 57	H	89.39	29.45 ||||	-0.18
H:TYR 58		112.70	45.73 |||||	0.61
H:HIS 59		47.52	26.93 ||||||	-0.49
H:TRP 64		191.71	19.44 ||	0.04
ZM109:SIA 582-PG16:L	H	436.88	76.46 ||	-1.12
L:ARG 94	H	168.75	28.25 ||	-0.35
L:HIS 95A	H	86.96	22.74 |||	0.31

Bond type: H: **H**ydrogen, S: **S**alt bridge
ASA Accessible Surface Area, $Å^2$
BSA BuriedSurfaceArea,$Å^2$
$\Delta_i G$ Solvation energy effect, kcal/mol
|||| Buried area percentage, one bar per 10%
Detailed interface data was calculated on the EBI PISA server (http://www.ebi.ac.uk/msd-srv/prot_int/cgi-bin/piserver)

D. Hydrogen bonds interactions between glycans and PG16 or PG9

Glycan residue	PG16 residue	distance	PG9 residue	distance
Nag 560 O5	His $100B_{HC}$ NE2	**3.07**	Arg $100B_{HC}$ NH2	**3.29**
Nag 560 O6			Arg $100B_{HC}$ NH2	**2.98**
			Asp 100_{HC} OD2	**2.62**
			Arg $100B_{HC}$ NE	**3.08**
Man 565 O2	Asp 31_{LC} O	**2.67**	Glu 31_{LC} O	**2.72**
	Asp 50_{LC} OD1	**3.38**	Asp 50_{LC} OD1	**3.36**
	Asp 50_{LC} OD2	3.89	Asp 50_{LC} OD2	3.54
Man 565 O3	Asp 31_{LC} O	3.63	Glu 31_{LC} O	3.6
	Asp 50_{LC} OD1	**2.57**	Asp 50_{LC} OD1	**2.7**
	Ser 32_{LC} OG	**2.95**	Ser 32_{LC} OG	**2.74**
	His $100R_{HC}$ ND1	**3.02**	His $100R_{HC}$ ND1	**2.89**
	Tyr $100Q_{HC}$ O	3.79	Tyr $100Q_{HC}$ O	3.81
Man 565 O4	His $100R_{HC}$ ND1	3.68	His $100R_{HC}$ ND1	3.69
Man 566 O3	Asn $100P_{HC}$ N	**3.11**	Asn $100P_{HC}$ N	**2.9**
	Asn $100P_{HC}$ ND2	3.72	Asn $100P_{HC}$ ND2	**3.37**
Man 566 O4	His $100R_{HC}$ NE2	**2.79**	His $100R_{HC}$ NE2	**2.79**
	Asn $100P_{HC}$ ND2	**3.39**	Asn $100P_{HC}$ ND2	**3.12**

Glycan residue	PG16 residue	distance	PG9 residue	distance
Nag 573 N2			Tyr $100K_{HC}$ OH	3.81
Nag 573 O7			Tyr $100K_{HC}$ OH	**2.94**
Gal 581 O4	Arg 94_{LC} NH2	3.86		
Gal 581 O6	Trp 64_{HC} NE1	3.84		
Sia 582 N5	Lys 57_{HC} O	**3.08**		
Sia 582 O1	His 59_{HC} N	**3.13**		
	His 59_{HC} ND1	3.94		
	His 59_{HC} O	3.61		
Sia 582 O3	His 59_{HC} ND1	**2.75**		
Sia 582 O8	His 95_{LC} NE2	**3.03**		
Sia 582 O9	Arg 94_{LC} O	**2.68**		
	Arg 94_{LC} NE	3.87		
	His 95_{LC} NE2	**3.39**		

Supplementary Table 3. Neutralization activity of PG9, PG16 and PG9,16-RSH on a large panel of pseudoviruses (195).

A. IC_{50} and IC_{80} neutralization for PG9,16-RSH, PG9 and PG16

		IC_{50}			IC_{80}		
Virus ID	**Clade**	**PG9,16-RSH**	**PG9**	**PG16**	**PG9,16-RSH**	**PG9**	**PG16**
0260.v5.c36	A	0.702	1.120	2.090	6.060	8.410	>50
0330.v4.c3	A	0.003	0.013	0.002	0.016	0.038	0.014
0439.v5.c1	A	>50	>50	>50	>50	>50	>50
3365.v2.c20	A	0.011	0.060	0.005	0.111	0.233	0.064
3415.v1.c1	A	0.038	0.096	0.021	0.190	0.540	0.157
3718.v3.c11	A	0.009	0.038	0.012	0.038	0.136	0.079
398-F1_F6_20	A	>50	>50	>50	>50	>50	>50
BB201.B42	A	0.002	0.007	0.001	0.006	0.026	0.005
BB539.2B13	A	0.007	0.054	0.007	0.038	0.163	0.025
BI369.9A	A	0.003	0.017	0.004	0.020	0.067	0.022
BS208.B1	A	0.001	0.008	0.001	0.006	0.027	0.005
KER2008.12	A	0.002	0.007	0.002	0.010	0.028	0.016
KER2018.11	A	0.002	0.008	0.001	0.009	0.029	0.004
KNH1209.18	A	0.106	0.180	0.421	>50	>50	>50
MB201.A1	A	0.033	0.103	0.021	0.130	0.305	0.224
MB539.2B7	A	0.011	0.060	0.010	0.073	0.256	0.150
MI369.A5	A	0.020	0.050	0.008	0.135	0.226	0.300
MS208.A1	A	0.031	0.079	0.030	0.279	0.609	>50
Q23.17	A	0.001	0.003	*0.000*	0.004	0.012	0.002
Q259.17	A	0.023	0.050	0.031	0.186	0.340	28.500
Q769.d22	A	0.005	0.011	0.123	0.032	0.038	5.040
Q842.d12	A	0.009	0.024	0.003	0.029	0.068	0.022
QH209.14M.A2	A	>50	>50	>50	>50	>50	>50
RW020.2	A	0.081	0.124	0.253	1.090	0.771	27.900
UG037.8	A	0.007	0.014	0.002	0.037	0.080	0.015
3301.V1.C24	AC	0.091	0.230	0.011	0.610	1.400	0.134
3589.V1.C4	AC	0.006	0.027	0.522	0.034	0.098	>50
6540.v4.c1	AC	0.006	0.030	0.005	0.041	0.105	0.080
6545.V4.C1	AC	0.006	0.036	0.016	0.043	0.144	0.315
0815.V3.C3	ACD	>50	>50	>50	>50	>50	>50
6095.V1.C10	ACD	0.126	0.151	0.011	1.630	1.130	0.157
3468.V1.C12	AD	0.888	1.620	0.885	>50	>50	>50
Q168.a2	AD	0.021	0.060	0.008	0.079	0.179	0.043
Q461.e2	AD	0.898	2.050	5.120	5.860	15.600	>50
620345.c1	AE	1.690	1.010	>50	>50	>50	>50
BJOX009000.02.4	AE	0.976	1.940	4.880	3.980	7.730	>50
BJOX010000.06.2	AE	0.110	0.303	13.400	0.759	1.550	>50
BJOX015000.11.5	AE						
BJOX025000.01.1	AE	0.204	0.096	0.431	1.960	0.826	>50
BJOX028000.10.3	AE	1.560	0.690	14.900	11.000	3.680	>50
C1080.c3	AE	0.001	0.002	*0.000*	0.002	0.008	0.002
C2101.c1	AE	0.007	0.031	0.006	0.052	0.139	0.300
C3347.c11	AE	0.006	0.030	0.005	0.034	0.103	0.028
C4118.09	AE	0.011	0.038	0.019	0.045	0.093	0.196
CM244.ec1	AE	0.001	0.004	0.001	0.003	0.014	0.003
CNE3	AE	0.035	0.064	0.059	0.501	0.598	>50
CNE5	AE	0.003	0.008	0.003	0.010	0.027	0.028

		IC$_{50}$			IC$_{80}$		
Virus ID	**Clade**	**PG9,16-RSH**	**PG9**	**PG16**	**PG9,16-RSH**	**PG9**	**PG16**
CNE55	AE	0.104	0.197	0.588	1.140	2.080	>50
CNE56	AE	>50	>50	>50	>50	>50	>50
CNE59	AE	0.068	0.060	0.028	0.764	0.443	4.460
CNE8	AE	1.240	0.980	0.675	9.000	4.850	>50
M02138	AE	0.065	0.210	0.050	0.468	0.954	1.000
R1166.c1	AE	0.568	1.100	0.414	2.260	3.900	7.640
R2184.c4	AE	0.247	0.384	3.680	1.570	2.230	>50
R3265.c6	AE	0.025	0.084	0.010	0.137	0.322	0.091
TH023.6	AE	0.064	0.138	4.160	2.960	7.890	>50
TH966.8	AE	0.006	0.015	0.002	0.028	0.061	0.010
TH976.17	AE	>50	>50	>50	>50	>50	>50
235-47	AG	0.047	0.124	0.064	0.563	0.803	4.650
242-14	AG	0.017	0.048	0.015	0.071	0.151	0.924
263-8	AG	0.135	0.211	0.551	0.779	1.270	12.200
269-12	AG	0.551	1.420	0.172	1.930	5.170	1.100
271-11	AG	0.010	0.059	0.101	0.300	0.948	>50
928-28	AG	0.004	0.038	0.016	0.030	0.225	0.115
DJ263.8	AG	0.045	0.091	0.042	0.344	0.551	8.990
T250-4	AG	*0.000*	0.001	*0.000*	0.001	0.004	0.002
T251-18	AG	>50	>50	5.620	>50	>50	>50
T253-11	AG	0.056	0.142	2.860	0.570	0.819	>50
T255-34	AG	0.011	0.020	0.006	0.095	0.126	0.073
T257-31	AG	0.006	0.019	0.002	0.025	0.059	0.011
T266-60	AG	0.129	0.321	0.482	0.908	1.420	13.800
T278-50	AG	0.329	0.385	0.381	2.170	2.510	21.000
T280-5	AG	0.119	0.339	0.273	0.504	1.060	4.870
T33-7	AG	0.004	0.019	0.016	0.034	0.162	0.471
3988.25	B	0.012	0.045	0.022	0.078	0.200	0.841
5768.04	B	0.114	0.270	0.285	2.940	2.540	>50
6101.10	B	>50	>50	>50	>50	>50	>50
6535.3	B	0.125	0.166	4.180	0.917	1.220	>50
7165.18	B	>50	>50	12.200	>50	>50	>50
45_01dG5	B	0.030	0.128	0.015	0.187	0.414	0.069
89.6.DG	B	>50	>50	>50	>50	>50	>50
AC10.29	B	0.007	0.031	0.005	0.051	0.191	0.060
ADA.DG	B	0.097	0.216	0.010	7.320	>50	>50
Bal.01	B	0.334	0.569	>50	8.590	>50	>50
BaL.26	B	0.009	0.030	0.405	0.186	0.356	>50
BG1168.01	B	>50	>50	>50	>50	>50	>50
BL01.DG	B	>50	>50	>50	>50	>50	>50
BR07.DG	B	>50	>50	>50	>50	>50	>50
BX08.16	B	0.004	0.017	0.010	0.038	0.101	25.000
CAAN.A2	B	2.850	6.310	11.000	>50	>50	>50
CNE10	B	0.095	0.222	>50	0.575	1.680	>50
CNE12	B	>50	>50	>50	>50	>50	>50
CNE14	B	>50	>50	>50	>50	>50	>50
CNE4	B	>50	>50	>50	>50	>50	>50
CNE57	B	>50	>50	>50	>50	>50	>50
HO86.8	B	0.006	0.051	0.005	0.137	0.345	0.051
HT593.1	B	0.213	0.345	0.150	3.680	4.050	11.900
HXB2.DG	B	0.207	1.000	>50	4.110	40.000	>50
JRCSF.JB	B	0.001	0.004	0.003	0.005	0.016	0.076

			IC_{50}				IC_{80}	
Virus ID	**Clade**	**PG9,16-RSH**	**PG9**	**PG16**	**PG9,16-RSH**	**PG9**	**PG16**
JRFL.JB	B	>50	>50	>50	>50	>50	>50
MN.3	B	3.570	17.100	>50	>50	>50	>50
PVO.04	B	3.530	7.630	10.100	13.700	20.700	>50
QH0515.01	B	>50	>50	>50	>50	>50	>50
QH0692.42	B	>50	>50	>50	>50	>50	>50
REJO.67	B	0.002	0.006	0.006	0.020	0.056	5.000
RHPA.7	B	4.600	9.970	0.465	32.100	>50	4.730
SC422.8	B	0.241	0.542	3.180	8.170	18.100	>50
SF162.LS	B	>50	>50	>50	>50	>50	>50
SS1196.01	B	0.020	0.147	0.017	0.338	1.150	0.935
THRO.18	B	4.570	4.870	0.809	>50	>50	>50
TRJO.58	B	0.047	0.173	0.766	0.623	1.810	38.800
TRO.11	B	9.110	>50	3.250	>50	>50	>50
WITO.33	B	0.002	0.007	0.002	0.008	0.020	0.011
YU2.DG	B	1.940	2.080	0.150	>50	>50	16.800
CH038.12	BC	3.690	5.530	5.580	>50	>50	>50
CH070.1	BC	0.001	0.006	0.002	0.004	0.018	0.008
CH117.4	BC	0.001	0.006	0.004	0.003	0.020	0.029
CH181.12	BC	0.001	0.004	0.001	0.006	0.019	0.003
CNE15	BC	0.001	0.005	0.001	0.004	0.018	0.006
CNE19	BC	0.004	0.015	0.035	0.028	0.068	1.980
CNE20	BC	0.038	0.047	3.220	0.188	0.163	>50
CNE21	BC	0.033	0.063	0.120	0.191	0.397	20.200
CNE40	BC	0.731	0.812	6.930	9.870	7.710	>50
CNE7	BC	0.394	1.020	0.148	1.860	4.280	1.750
286.36	C	0.091	0.185	0.024	0.300	0.668	0.071
288.38	C	3.300	2.420	0.564	>50	>50	>50
0013095-2.11	C	0.004	0.012	0.007	0.023	0.074	0.044
001428-2.42	C	0.001	0.002	*0.000*	0.003	0.007	0.002
0077_V1.C16	C	0.027	0.083	0.006	0.116	0.342	0.027
00836-2.5	C	>50	>50	>50	>50	>50	>50
0921.V2.C14	C	0.001	0.004	0.001	0.003	0.012	0.003
16055-2.3	C	0.003	0.016	0.002	0.013	0.037	0.010
16845-2.22	C	2.410	1.960	1.760	44.300	>50	>50
16936-2.21	C	>50	>50	>50	>50	>50	>50
25710-2.43	C	0.007	0.031	0.003	0.068	0.139	0.191
25711-2.4	C	0.460	0.932	0.018	1.750	3.690	0.235
25925-2.22	C	0.007	0.025	0.004	0.028	0.071	0.022
26191-2.48	C	0.106	0.132	0.390	0.950	0.809	>50
3168.V4.C10	C	0.043	0.092	0.025	0.150	0.393	0.201
3637.V5.C3	C	>50	>50	>50	>50	>50	>50
3873.V1.C24	C	>50	>50	>50	>50	>50	>50
6322.V4.C1	C	>50	>50	>50	>50	>50	>50
6471.V1.C16	C	>50	>50	>50	>50	>50	>50
6631.V3.C10	C	>50	>50	>50	>50	>50	>50
6644.V2.C33	C	0.003	0.025	>50	0.029	0.103	>50
6785.V5.C14	C	0.001	0.008	0.002	0.007	0.043	0.020
6838.V1.C35	C	*0.000*	0.006	0.001	0.003	0.032	0.004
96ZM651.02	C	>50	>50	>50	>50	>50	>50
BR025.9	C	0.004	0.019	0.004	0.022	0.065	0.024
CAP210.E8	C	0.057	0.165	0.023	0.412	0.876	0.736
CAP244.D3	C	0.017	0.067	0.009	0.102	0.231	0.037

			IC_{50}				IC_{80}		
Virus ID	**Clade**		**PG9,16-RSH**	**PG9**	**PG16**		**PG9,16-RSH**	**PG9**	**PG16**
CAP45.G3	C		*0.000*	0.003	0.001		0.002	0.010	0.002
CNE30	C		>50	>50	>50		>50	>50	>50
CNE31	C		19.700	15.800	3.190		>50	>50	>50
CNE53	C		0.054	0.080	>50		0.235	0.430	>50
CNE58	C		0.007	0.022	0.004		0.035	0.064	0.019
DU123.06	C		0.030	0.062	0.010		0.154	0.315	0.064
DU151.02	C		0.003	0.016	0.002		0.016	0.054	0.007
DU156.12	C		0.014	0.041	0.003		0.079	0.143	0.016
DU172.17	C		0.071	0.190	0.015		0.278	0.758	0.080
DU422.01	C		>50	>50	>50		>50	>50	>50
MW965.26	C		0.860	0.619	0.123		>50	26.000	>50
SO18.18	C		0.006	0.021	0.003		0.033	0.065	0.021
TV1.29	C		0.002	0.005	0.002		0.008	0.027	0.050
TZA125.17	C		0.034	0.140	0.031		0.281	0.808	1.960
TZBD.02	C		0.032	0.170	0.010		0.215	0.676	0.082
ZA012.29	C		9.120	7.470	4.770		>50	>50	>50
ZM106.9	C		0.526	0.492	0.482		6.290	4.190	>50
ZM109.4	C		0.041	0.154	10.000		0.502	2.440	>50
ZM135.10a	C		>50	>50	>50		>50	>50	>50
ZM176.66	C		0.003	0.010	0.001		0.012	0.033	0.005
ZM197.7	C		0.164	0.369	0.434		1.100	2.130	9.790
ZM214.15	C		>50	>50	>50		>50	>50	>50
ZM215.8	C		0.065	0.073	>50		0.517	0.497	>50
ZM233.6	C								
ZM249.1	C		0.015	0.043	0.013		0.209	0.267	1.820
ZM53.12	C		0.020	0.036	0.003		0.106	0.129	0.020
ZM55.28a	C		5.370	3.150	>50		>50	>50	>50
3326.V4.C3	CD		0.009	0.030	0.011		0.053	0.103	0.094
3337.V2.C6	CD		>50	>50	>50		>50	>50	>50
3817.v2.c59	CD		0.001	0.004	0.002		0.003	0.015	0.016
191821.E6.1	D		1.810	5.540	>50		>50	>50	>50
231965.c1	D		0.845	0.682	2.540		>50	>50	>50
231966.c02	D								
247-23	D		0.075	0.092	4.230		0.441	0.422	>50
3016.v5.c45	D		0.207	0.283	>50		16.900	12.600	>50
57128.vrc15	D		0.035	0.122	0.137		0.356	0.465	>50
6405.v4.c34	D		>50	>50	>50		>50	>50	>50
A03349M1.vrc4a	D		>50	>50	>50		>50	>50	>50
A07412M1.vrc12	D		1.140	0.773	5.970		>50	17.900	>50
NKU3006.ec1	D		>50	>50	>50		>50	>50	>50
UG021.16	D								
UG024.2	D		6.070	2.420	>50		>50	>50	>50
P0402.c2.11	G		0.940	0.502	0.092		18.100	6.150	20.300
P1981.C5.3	G		0.085	0.201	0.953		2.100	2.680	>50
X1193.c1	G		0.036	0.120	0.016		0.145	0.378	0.115
X1254.c3	G		0.019	0.035	0.011		0.135	0.125	0.106
X1632.S2.B10	G		0.043	0.087	0.007		0.484	0.849	0.102
X2088.c9	G		>50	>50	>50		>50	>50	>50
X2131.C1.B5	G								
SIVmac251.30.SG3	NA		>50	>50	>50		>50	>50	>50
SVA.MLV	NA		>50	>50	>50		>50	>50	>50

B. IC_{50} and IC_{80} statistics on a panel of 195 isolates

	PG9,16-RSH	PG9	PG16
# Viruses	195	195	195
Total VS Neutralized			
IC50 <50ug/ml	157	156	147
IC50 <1ug/ml	138	133	122
% VS Neutralized			
IC50 <50ug/ml	81	80	75
IC50 <1ug/ml	71	68	63
Median IC50	0.033	0.082	0.018
Geometric Mean	0.038	0.093	0.042

	PG9,16-RSH	PG9	PG16
# Viruses	195	195	195
Total VS Neutralized			
IC80 <50ug/ml	139	137	103
IC80 <1ug/ml	108	100	77
% VS Neutralized			
IC80 <50ug/ml	71	70	53
IC80 <1ug/ml	55	51	39
Median IC80	0.145	0.315	0.080
Geometric Mean	0.155	0.311	0.136

C. Correlation between PG9,16-RSH improvement as a function of PG9 potency on 195 viruses.

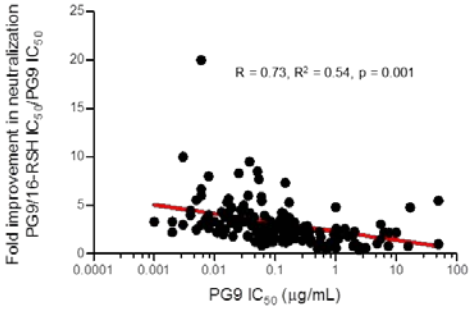

Supplementary Table 4. NMR chemical shifts

A. ^{1}H chemical shifts of complex-type glycan

Glycan rings	^{1}H chemical shifts							
	H1	H2	H3	H4	H5	H6/H6'	H9/H9'	Ac
A	4.955	3.747	3.646	3.544	3.471	3.524, 3.72		1.905
B	4.5403	3.677	3.646	3.612	3.494	3.524, 3.720		1.972
C	4.66	4.140	3.664	3.667	3.552	3.670, 3.843		
D	5.018	4.082	3.785	3.384	3.496	3.520, 3.757		
E	4.830	4.00	3.781	3.384	3.496	3.508, 3.786		
F	4.489	3.638	3.64	3.542	3.548	3.722, 3.860		1.958
G	4.333, 4.35	3.424	3.556	3.812	3.706	3.876, 3.431		
Sia			Ax,1.599 Eq, 2.552	3.539	3.688	3.581	3.585	1.92
Asn	3.799	2.776, 2.683						

B. ^{13}C chemical shifts of complex-type glycan

Glycan rings	^{13}C chemical shifts							
	C1	C2	C3	C4	C5	C6	C9	Ac
A	77.94	53.46	72.67	78.5	76.06	59.74		21.95
B	101.18	54.80	71.92	79.49	74.31	59.85		21.95
C	100.32	70.14	80.36	65.52	74.17	65.77		
D	99.41	76.25	69.301	67.15	72.71	62.51		
E	96.82	76.08	69.32	67.15	72.71	61.53		
F	99.18	54.50	71.95	80.56	74.3	60.11		22.14
G	103.42, 102.8	70.64	72.31	73.57	73.57	63.21		
Sia			39.94	68.12	51.76	72.41	69.47	22.34
Asn	51.07	35.67						

C. ^{1}H chemical shifts of $Man_5GlcNAc_2$

Glycan rings	^{1}H chemical shifts					
	H1	H2	H3	H4	H5	H6, H6'
Aα	5.063	3.752	3.762	3.505	3.755	
Aβ	4.51	3.573	3.551	3.495	3.385	3.521, 3.708
B	4.521	3.703	3.698	3.653	3.520	
C	4.702	4.171	3.685	3.709	3.560	3.875/3.696
D	4.792	4.065	3.840	3.785	3.772	3.9109, 3.660
E	5.0143	3.990	3.809	3.555	3.733	3.660, 3.831
F	5.001	3.985	3.809	3.57	3.696	3.687, 3.807
G	4.826	3.904	3.752	3.591	3.608	

Individual rings are labeled as shown in Fig. 5b.

D. ^{13}C chemical shifts of $Man_5GlcNAc_2$

Glycan rings	^{13}C chemical shifts					
	C1	C2	C3	C4	C5	C6
Aα	90.27	53.52	69.12	79.58	69.2	
Aβ	94.68	55.94	72.38	79.13	74.44	59.95
B	101.31	54.89	71.924	79.48	74.44	
C	100.34	70.14	80.56	65.42	74.31	65.93
D	99.8	69.38	78.57	65.59	70.78	65.131
E	102.44	69.95	70.3	66.81	77.81	61.067
F	102.2	70.05	70.3	66.7	73.26	60.94
G	99.2	69.88	70.52	66.66	72.64	

Individual rings are labeled as shown in Fig. 5b.

Supplementary Note

ELISAs. *PG9 and PG16 detection.* 2µg/mL of scaffolded V1/V2 were coated overnight in PBS at 4ºC. Plates were washed once with PBS tween 0.2% and blocked for 2 hours at room temperature (5% skim milk in PBS). Antibodies (PG9 and PG16) were added starting at 10µg/ml with 5-fold dilution in PBS tween 0.2% for 1 hour. Plates were washed 5 times in PBS tween 0.05%. Secondary antihuman peroxidase conjugate antibody at 1:5,000 dilution was added to the plate for1 hour. The plates were washed 5 times in PBS Tween 0.05%. Plates were developed using 3,3´,5,5´-tetramethylbenzidine (TMB) (Kirkegaard & Perry Laboratories) for 10 minutes and the reaction was stopped with 180nM H2SO4. The readout was measured at a wavelength of 450nm. All samples were tested in duplicate**.** *Lectin detection.* Scaffolded-V1/V2 was coated overnight in PBS at 4ºC. Wells were blocked using Carbo free block from Vector Biolaboratories. Biotinylated lectins were added to the wells for 1 hour at RT in PBS tween 0.2% and then washed 5 times in PBS tween 0.05%. Vecstatin was added for 1 hour at RT. Plates were washed in PBS Tween 0.05% and developed using TMB. The average absorbance over multiple wells after subtraction of background reactivity is shown for each lectin with standard deviations from the mean as error bars. Some background noise was observed for SN lectin binding to the plate. Sambucus nigra lectin (S)N binds preferentially to Sia(α2-6)Gal, and to a lesser degree Sia(α2-3)Gal. Maackia amurensis lectin II (MA) prefers to bind sialic acid in an (α2-3) linkage. CVN recognizes any glycans that contain α1-2 linked – mannobiose, which are present on Man-7 through Man-9. Con A interacts with branched α-mannosides present in high-mannose type, hybrid type and biantennary complex type *N*-glycans.